PHOTOTHYRISTORS

A photothyristor can be broadly defined as a thyristor capable of optically controlled switching. Other names used for photothyristors include optical thyristor and optothyristor. Depending on the detailed design and application, a photothyristor, when switched on, may emit light either spontaneously or in response to a stimulus.

The basic structure of a thyristor is formed by four layers of alternatively doped *pnpn* semiconductors. A traditional thyristor generally has three terminals, called anode, cathode, and gate, as shown in Fig. 1(a). The gate terminal can be attached to either the central $n1$ or $p2$ region. A thyristor can be viewed as consisting of two bipolar transistors, one p^+1n1p2 and one n^+2p2n1 as shown in Fig. 1(b).

When a reverse bias voltage is applied to a thyristor by holding the cathode to a higher voltage with respect to the anode, the J1 and J3 junctions become reverse biased. Because a reverse biased p–n junction can conduct only a very small junction leakage current, a reverse biased thyristor will, therefore, be in a high impedance OFF state; addition-

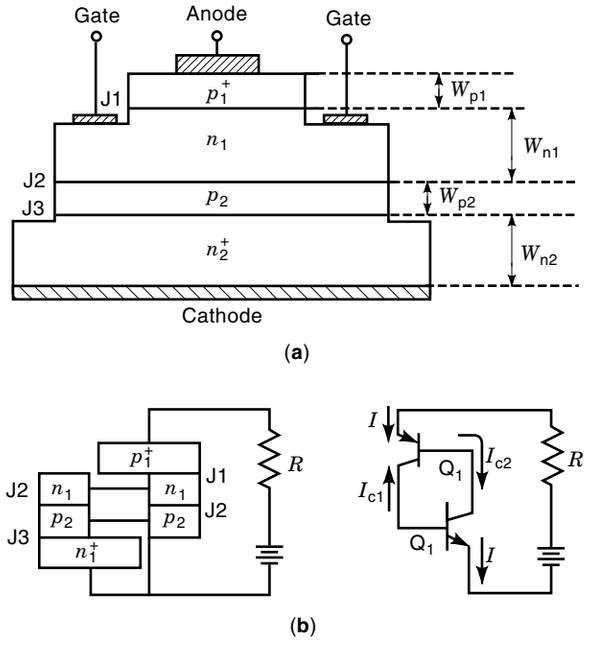

Figure 1. The cross-sectional view of a thyristor (a) and the two-bipolar-transistor-equivalent circuit of the thyristor (b).

ally, only a small leakage current can flow through the thyristor until the reverse bias voltage is so high that both of the reverse biased junctions break down due to avalanche or impact ionization.

Avalanche breakdown occurs when the electric field across the semiconductor exceeds its critical field strength. In this case, the carriers, namely, the electrons and holes that carry the small leakage current, gain enough kinetic energy from the applied electric field to knock out bound electrons, thereby creating more free carriers for current conduction. These carriers can repeat the same impact ionization process to knock out more carriers while moving through the reverse biased junctions, which leads to an avalanche process that causes the breakdown of a *pn* junction.

When a thyristor is forward biased, however, both J1 and J3 junctions become forward biased and the J2 junction becomes reverse biased. The two transistors p^+1n1p2 and n^+2p2n1 are both operating in the active amplifying mode because the emitters and collectors are forward and reverse biased, respectively. If the forward bias across the thyristor is increased, the forward bias across the p^+1n1 and n^+2p2 junctions will also increase, leading to increased hole injection from p^+ into $n1$ and electron injection from n^+2 into $p2$. The injected electrons from the cathode n^+2 region will diffuse across the $p2$ base region and enter the reverse biased $n1$-drift region, where they are swept through by the applied electric field into the $n1$ neutral region (this is the base region of the p^+1n1p2 transistor). Once these electrons enter this $n1$ base region, they act as the base current for the p^+1n1p2 transistor, which causes more holes to be injected from the p^+1 anode. This results in the well-known bipolar transistor action. Similarly, these emitted holes will diffuse through the $n1$ base region and be swept by the applied electric field through the depleted J2 region into the $p2$ base of the n^+2p2n1 transistor, which acts as the base current and forces more electrons to be injected from n^+2 into $p2$ region.

This regenerative process can continue to build up if the applied voltage is large enough until the concentration of the emitted electrons and holes in the central $n1$ and $p2$ regions are so high that the J2 junction can no longer support a reverse bias. The voltage across the J2 junction, and hence the voltage across the thyristor then collapses, leading to the ON state of the thyristor, in which the central $p2$ and $n1$ regions are flooded with electron and hole plasma and a large current conducts through the thyristor. In the ON state, all three junctions are forward biased. However, due to the high concentrations of electrons and holes injected into the center $n1$ and $p2$ regions, a photothyristor in the ON state can be regarded as a *p-i-n* diode ("*i*" is an intrinsic semiconductor in which equal concentrations of electrons and holes exist).

Figure 2 shows a typical thyristor current–voltage characteristics. After turning on, the thyristor stays in the low impedance ON state until either the current through the thyristor is reduced to below a certain minimum value called the holding current I_H or the voltage across the thyristor is reduced to below the holding voltage V_H. When the ON-state current or voltage falls below I_H or V_H, the thyristor returns back to the OFF state because the base currents due to the injection of electrons and holes are not large enough to maintain the regenerative process. The required base current to initiate and support the regenerative process for turning on the thyristor can be provided by the third gate terminal without increasing the forward bias to the breakdown voltage. This gate current is generally called triggering current. The larger the triggering current the lower the voltage at which the thyristor turns on.

Other key parameters for thyristor operation are shown in Fig. 2, where V_{BF} denotes the forward blocking voltage at zero gate bias. The value of V_{BF} depends on the doping concentrations and thicknesses of the two central layers, especially the lightly doped one. The current I_S corresponding to V_{BF} is called switching current or turn-on current. The reverse breakdown voltage of a thyristor is denoted V_{BR}.

A thyristor is therefore a switching device that can block a designed voltage with negligible current conduction in the forward blocking and reverse OFF states and can conduct a

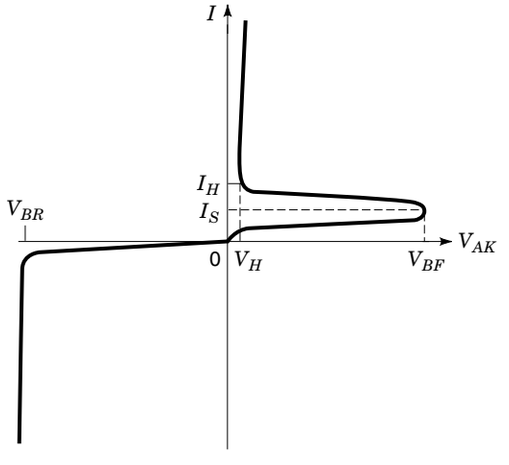

Figure 2. Typical current-voltage characteristics of a thyristor.

large current with small voltage drop across the switch in the forward ON-state. The turn-on of a thyristor can be accomplished by the gate triggering or by simply increasing the switch voltage to V_{BF}.

In a photothyristor, the base current needed to turn on the thyristor can be provided by absorbing light illuminated on the center region of the thyristor. When the photon energy of the optical beam is equal to or larger than the energy bandgaps of the center $n1$ and $p2$ semiconductors, optical photons are absorbed effectively by the semiconductors to create free carriers of electrons and holes. These optically generated carriers are swept to the base regions of the two transistors in a photothyristor by the electrical field across the center J2 junction. They act as the base current to initiate and support the regenerative process needed to turn on a photothyristor. Because the optical absorption process is very fast and a very short optical pulse of high energy is available from solid state or semiconductor lasers, photothyristors could be operated at a much higher speed than conventional thyristors. The turn-off of a photothyristor can be accomplished by either reducing the forward current to below V_H.

A photothyristor is unique because it can produce light by either spontaneous or stimulated photon emission when correctly designed and operated in the ON state. Spontaneous emission generates noncoherent light while stimulated emission produces laser light, which is coherent. For example, when GaAs instead of Si is used, the high density of electrons and holes in the center $n1$ and $p2$ regions can be recombined radiatively, releasing the energy in the form of photons, the quanta of light energy. The radiative process dominates the electron and hole recombination in GaAs because it is a direct bandgap semiconductor whereas Si is an indirect bandgap semiconductor. A semiconductor is regarded as a direct bandgap semiconductor when the minimum energy position in the conduction band lines up, in the momentum space, with the maximum position of the valance band (1). In this case, electrons can recombine easily with a hole with the extra energy carried away by a photon while keeping the momentum conserved. This occurs because a photon has negligible momentum in comparison to an electron or a hole. In an indirect bandgap semiconductor such as Si, most of the electrons in the conduction band and the holes in the valance band have different momentum. An electron and a hole can not readily recombine to create a photon while keeping the momentum conserved. The extra energy released when an electron recombines with a hole in an indirect semiconductor is often carried away by phonons, the quanta of heat energy.

Light emission from a photothyristor operated in the ON state provides a new degree of freedom in achieving new applications. In the case of high power photothyristors, for instance, the spreading speed of electron and hole plasma, which determines the turn-on speed of photothyristors, can be much higher than the electron and hole carrier velocities due to photon-assisted generation and recombination. Basically, during the spreading of electron and hole plasma, the photons generated by electron and hole recombination travel at a much higher speed, the speed of light, through the junction. While spreading out at the speed of light, they can be reabsorbed in the process to generate electron and hole pairs. The net effect is that the electron and hole plasma spreads out at a speed higher than the carrier speed in the semiconductor, thus helping to turn on the photothyristor at a higher speed. For a low power photonic switching application, the spontaneous or the stimulated emission of light from a photothyristor makes it a unique device for many photonic applications, including optical computing, signal processing, and optical interconnections.

In the following description, a brief discussion of design and operation principles for the low power and high power photothyristors will first be presented, followed by a review of an analytical model that enables quick design and analysis of photothyristors including the forward breakover voltage and the ON-state voltage drop, which is largely responsible for the ON-state power dissipation. A general design and analysis model is then presented; it facilitates dc investigation of photothyristors for low- and high-power applications. An equivalent circuit model is then described; it facilitates ac analysis, multiple device modeling, and the inclusion of interaction of photothyristors with other devices and circuit elements.

BRIEF DESCRIPTION OF PHOTOTHYRISTORS

Low-Voltage Photothyristor

Figure 3(a) shows the energy band diagram for a *PnpN* AlGaAs/GaAs based low-power photothyristor under zero bias. The capital P and N represent the wider bandgap p-doped and n-doped AlGaAs semiconductors, respectively. The lower case n and p denote smaller bandgap n-type GaAs and p-type GaAs, respectively. The center n and p layers are not lightly doped in comparison to the outer P and N layers. This aids in reducing surface recombination current. Reduced surface recombination leads to an improved optical triggering sensitivity over that found in the conventional structures to be discussed in the example in a later section. One of the main reasons for the use of a wider bandgap AlGaAs is the

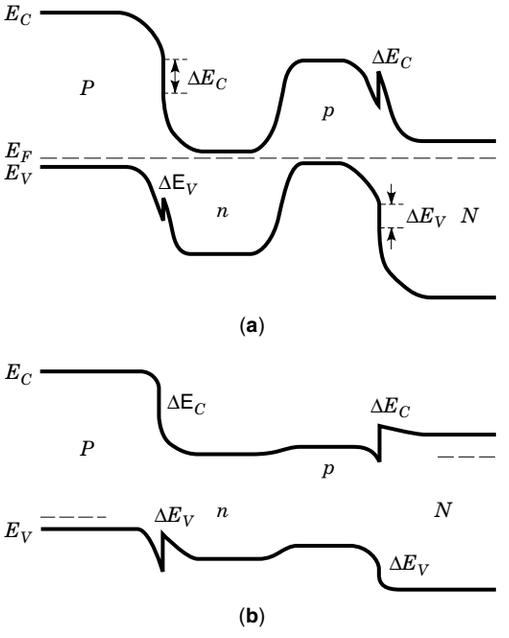

Figure 3. The energy band diagrams for a *PnpN* AlGaAs/GaAs based low-power photothyristor under zero bias (a) and in the ON state (b).

optical window effect it provides for optical illumination. The optical window effect refers to the fact that photons with energy around the bandgap energy of GaAs are not absorbable by the wider bandgap AlGaAs. This wider window makes it possible for the optical triggering energy to be largely absorbed by the reverse biased center J2 junction. For low-power photonic switching application, the center layer thicknesses of n and p are generally less than 1 μm so that the forward blocking voltage is typically a few volts, determined by either avalanche or punchthrough breakdown. In either case, the ramp rate of the forward bias voltage V must be kept below a certain value so as to avoid the undesired early turn-on of a photothyristor by dV/dt triggering (1). This dV/dt effect is caused by the rapidly varying anode voltage giving rise to a displacement current $d(CV)/dt$, where C is the J2 junction capacitance. This displacement current, when large enough, will initiate the positive regenerative process to turn on the photothyristor.

Once the photothyristor turns on, the center p and n layers are flooded with electron and hole pairs and the reverse bias in the center junction collapses. The *PnpN* structure operates like a *P-i-N* diode. If radiative recombination dominates in the center layers, a strong photon emission occurs. The photothyristor can be regarded as a light-emitting diode in the ON state if the spontaneous emission dominates. By improving confinement of electrons and holes as well as the optical field in the center region of a photothyristor, stimulated emission may be possible; thus the photothyristor functions, in this case, as a laser in the ON state. The wider bandgap used in the structure illustrated in Fig. 3(a) helps to confine electrons and holes in the same region, the "*i*" region, so that there is a greater chance that radiative recombination may occur, thereby producing more photons in comparison to the conventional homojunctions. To make this clear, the ON-state energy band diagram of the photothyristor is shown in Fig. 3(b). The band discontinuity between AlGaAs and GaAs in the conduction band and valance band are labeled ΔE_C and ΔE_V, respectively. They serve as energy barriers to prevent electrons and holes from escaping out of the center "*i*" region. In addition to this carrier confinement, the difference between the dielectric constants of AlGaAs and GaAs helps to confine the optical field inside the "*i*" region, making this device structure more likely to produce stimulated light output.

For practical use, a photothyristor is generally turned on either by a beam of light absorbed in the center layers or by the dV/dt triggering, depending on its applications. For low-power photonic applications, direct light triggering requires only one photothyristor to represent the complementary "0" and "1" logic states (by using ON and OFF states); however, direct optical triggering requires more optical energy than dV/dt triggering. In a classic setup for direct light triggering, a forward bias V_A, slightly below the forward breakover voltage, is applied to the photothyristor through a current limiting resistor and a beam of light of suitable energy then illuminates the center junction to generate enough base current, in this way turning the photothyristor from OFF state to ON state. The I_{on} current is limited by the load resistance. The light output from this ON state may be used to trigger similar photothyristors from OFF state to ON state. This makes photothyristors useful devices for optical signal processing and computing.

In dV/dt triggering, however, two or more photothyristors are connected in parallel with a common external resistance R. The applied voltage is ramped quickly to turn on one of the photothyristors. Only one among the parallely connected photothyristors will be turned on by this dV/dt triggering because each photothyristor will always have a slightly different switching speed due to small differences among the photothyristors. The first photothyristor that turns on prevents the turn-on of all other competitors because of a quick bias voltage drop across the photothyristors due to the rapid increase in current and voltage across resistor R. Two similar photothyristors parallely connected in this manner form the so-called differential pair. The ON state of one of the photothyristors represents the logic "0" and the ON state of the other photothyristor the logic "1." When the two photothyristors are very much alike and no optical preillumination is applied, the winner is randomly chosen. A very low level preillumination, however, is sufficient to determine the winner in the pair. For this reason, dV/dt triggering using a differential pair is several orders of magnitude more sensitive to optical triggering when compared to the switching of a single photothyristor by optical illumination. The second advantage is that no critical V_A bias slightly below the breakover voltage is required. The third advantage is that Boolean information is transmitted in dual-rail code, namely, the photothyristor pair emits a signal for the transmission of both "0" and "1," which is known to improve the bit-error rate (BER) for transmission significantly. All of these occur at the expense of the requirement of an electrical clocking signal for synchronization. Of course, one more photothyristor is also required than is needed for the direct light-triggering approach.

A low power photothyristor possesses the following features that make it a potential candidate for many photonic applications: (1) its logic states or ON and OFF states are optically or electrically controllable; (2) its differential pair makes dual rail logic possible with all the performance benefits of differential operation; (3) when hybridly combined with Si chips, it allows for the construction of smart pixels; and (4) it is relatively simple to form 2-D arrays, especially with the two-terminal photothyristors. The key parameters for photothyristors to gain energy needed for switching, the electrical to optical energy conversion efficiency, and the characteristic of the emitted light, which controls the cascadability of photothyristor technology.

Low-power photothyristors, which combine the functions of receiving, transmitting, and memory into a single device while providing a large optical gain, are becoming a serious candidate for applications in the area of optical signal processing and photonic computing. A variety of low-power photothyristors are under active development and a few different names have been applied to the low-power photothyristor, including Double Heterostructure Optoelectronic Switch (DOES) (2), Vertical-to-Surface Transmission Electro-Photonic device (VSTEP) (3), and Ledistor (4). It is possible to design the *pnpn* structure such that when the device turns on it operates as a semiconductor *pn* junction laser. Such a negative differential laser based on *pnpn* four-layer structure has been called NDR laser (5) or Lasistor (4).

High Voltage Photothyristors

One of the key differences between the low- and high-power photothyristors lies in the center J2 junction. In a high-power photothyristor, the center J2 junction is designed to be capable of blocking high voltages by either increasing the $n1$ layer

thickness while decreasing its doping concentration or increasing the $p2$ layer thickness while decreasing its doping concentration. In the former case, the photothyristor is called an n-blocking photothyristor; in the latter case it is said to be a p-blocking device. Other than the critical parameter of forward voltage blocking capability, the ON-state voltage drop is another key parameter that serves to dominate the power dissipation in the ON-state.

Higher turn-on and turn-off speeds are the other two basic parameters of considerable design consideration. The Si-based light-triggered power thyristor has been investigated for many years and commercial systems are now entering the market. To improve speed performance, operable temperature range, and power capability for impulse applications, advanced semiconductor materials such as GaAs, AlGaAs, SiC and GaN can be used. These advanced materials have a larger bandgap, a higher carrier saturation velocity, a higher critical electric field strength and, in the case of SiC, a higher thermal conductivity than that of Si. All are highly desirable for power photothyristor applications. While a larger bandgap leads to high operating temperatures, a higher carrier saturation velocity leads to higher speed operation. Furthermore, higher thermal conductivity provides a faster way to remove the inevitably large amount of heat generated in a power device. Finally, a higher critical electric field strength allows for the fabrication of higher-power devices using the same thickness for the blocking layer in the center junction.

For photothyristor operation, however, another critical issue is the ability to sensitively trigger on the device without excessive optical power. To illustrate the issue of optical triggering, consider a high-power photothyristor shown in Fig. 4 based on semiconductors of AlGaAs and GaAs. The structure is composed of P^+n-i-pN^+ where the use of GaAs permits the device operation at higher temperatures in comparison to Si-based devices because the GaAs energy bandgap (1.43 eV) is larger than the bandgap of Si (1.12 eV). The use of undoped "intrinsic" bulk GaAs makes it possible for the photothyristor to block a very high voltage. AlGaAs with an even wider bandgap compared to GaAs is used as optical windows for efficient light illumination. This window action eliminates light absorption near the device surface, where absorption tends to cause slow turn on and increases required optical energy for triggering.

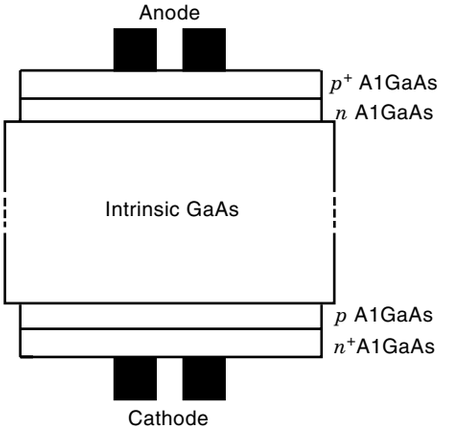

Figure 4. The cross-sectional view of an AlGaAs/GaAs based high-power photothyristor with a thick intrinsic or semiinsulating GaAs "inserted" into the conventional *PNPN* thyristor structure.

One of the key parameters affecting the hold-on voltage of a photothyristor with a given blocking voltage capability is the quality of the undoped GaAs and its thickness. High-quality undoped GaAs reduces the effect of deep levels and other defects, which has been argued to cause the lock-on phenomena (6) in photothyristor or bulk semiinsulating GaAs switches. If the undoped GaAs region is thicker than is required to block a given voltage, the ON-state voltage drop is not minimized, which results in extra undesirable power dissipation. When a positive high voltage is applied to the P^+ anode, the center n-i-p junction becomes reverse biased and most of the applied voltage is supported by the n-i-p junction. The photothyristor will be turned on under two conditions when no gate bias is applied. The first is punchthrough breakdown where the n or p region is completely depleted as a result of an applied electrical field. The second is avalanche breakdown, which occurs when the applied electric field is higher than the critical field of GaAs. In practical applications, a power photothyristor is biased slightly below the forward breakdown. Upon light illumination, a base current is generated as a result of photon absorption. If the generated base current is large enough, the establishing of positive feedback quickly leads to the turn on of the photothyristor.

DETAILED DESCRIPTION OF PHOTOTHYRISTORS

A Simplified Model for Photothyristor Design

A photothyristor has four modes of operation: forward blocking or high impedance OFF state; forward ON state; reverse OFF state; and reverse breakdown. In the reverse OFF state, only small leakage current conducts because junctions J1 and J3 are both reverse biased. The leakage current can be approximately described by (1)

$$I_{RL} = q\sqrt{D_p/\tau_p}\frac{n_i^2}{n1} + \frac{qn_i x_d}{2\tau_o} \tag{1}$$

where D_p is the hole diffusion constant, τ_p the low-level hole minority carrier lifetime in the most likely doped n-base, $n1$ the doping concentration, n_i the intrinsic carrier concentration, x_d the total depletion width of junction J1, and τ_0 the space charge lifetime. The first term describes the minority carrier drift current and the second term depicts the generation current in the space charge region.

In the forward blocking mode, the anode is positive with respect to the cathode so that only J2 junction is reverse biased. To understand the operation, let us consider the two-transistor model approximation of the photothyristor shown in Fig. 1(b). Because both transistors are biased in the forward active mode, the leakage current, which increases with the forward bias across the photothyristor, acts as the base current of the complementary transistor; this causes a positive feedback and leads to the turn on of the photothyristor. The condition under which forward turn on occurs can be found from the equivalent circuit shown in Fig. 1(b). If α_{pnp} and α_{npn} are the common base current gains of p^+1n1p2 and n^+2p2n1 transistors, respectively, then

$$I_{C1} = -\alpha_{pnp}I + I_{CO1} \tag{2}$$

and

$$I_{C2} = \alpha_{npn} I + I_{CO2} \tag{3}$$

where I_{CO1} and I_{CO2} are the saturation currents of the collector junctions of $p1n1p2$ and $n2p2n1$ transistors, respectively. As the total currents flowing into transistor $p1n1p2$ must be equal to zero, we have

$$I + I_{C1} - I_{C2} = 0 \tag{4}$$

Combining the preceding three equations results in

$$I = \frac{I_{CO2} - I_{CO1}}{1 - (\alpha_{pnp} + \alpha_{npn})} \tag{5}$$

Because α_{pnp} and α_{npn} are strong functions of current they increase with increased forward bias or increased light absorption until $\alpha_{pnp} + \alpha_{npn}$ approaches unity to turn on the photothyristor. Detailed analysis shows that the turn-on condition is that the sum of the small signal common base current gains for the two transistors approaches unity (1).

The forward breakover voltage of a photothyristor without light triggering can be easily calculated by assuming that most of the applied voltage is dropped across the center pn junction. Given the doping concentration $n1 \ll p2$, the avalanche forward breakover voltage can be calculated by

$$V_{\mathrm{BF}} = \frac{k_s \epsilon_0 E_c^2}{2qn1} \tag{6}$$

where k_s is the semiconductor relative dielectric constant, ϵ_0 the free space permittivity, q the electronic charge, and E_c the semiconductor critical avalanche field.

The breakover voltage is reached when the electric field reaches the critical avalanche field of the semiconductor. However, if the depletion width on either side of the center pn junction becomes equal to the corresponding layer width before the critical field is surpassed, breakover occurs by punchthrough. The depletion width on the relatively lightly doped side of the center pn junction can be calculated by

$$x_n = \sqrt{(2k_s\epsilon_0 V/(qn1)} \tag{7}$$

This is the equation for designing a punchthrough breakdown photothyristor.

Under light illumination, the blocking voltage of a photothyristor is reduced and the exact value of the blocking voltage can be numerically calculated. These conditions are a strong function of light intensity, semiconductor absorption coefficient, and carrier lifetime and mobility.

Once the photothyristor is operated in the forward ON state, the forward-biased p^+1n1 and n^+2p2 emitters inject high densities of electrons and holes, respectively, into the center layers. When the density of these excess carriers exceeds the background doping concentrations of the center layers an electron and hole plasma region is formed, making the photothyristor closely resemble a p-i-n diode. Depending on the level of carrier injection into the center base region, analytical models for the ON-state voltage drop V_{ON} of photothyristors have been developed. Because the power dissipation in the ON state relates directly to the ON-state voltage drop of the photothyristor, simplified models that can estimate the ON-state voltage drop become very useful. One such model is described next for a photothyristor formed by $p^{++}0p^+1n1p2n^+2$ five-layer structures (7).

First, for low-level injection, namely, when

$$J < \frac{qn1D_p}{L_p} \tag{8}$$

and

$$1 \gg \frac{\mu_p W_{p2} p2}{\mu_n W_{n2} n2} \tag{9}$$

the ON-state voltage drop is determined by

$$V_{\mathrm{ON}} = \frac{kT}{q} \ln \frac{W_{p2} p2 J}{qD_n n_i^2} \tag{10}$$

The moderate-level injection dominates when

$$1 \gg \frac{\mu_p W_{p2} p2}{\mu_n W_{n2} n2} \tag{11}$$

and

$$J < \frac{qp2D_p b}{W_{p2}} \tag{12}$$

In this case, the ON-state voltage drop is

$$V_{\mathrm{ON}} = \frac{kT}{q} \ln \frac{W_{p2} p2 J}{qD_n n_i^2} + \frac{kT}{q} \frac{b}{b+1} \left(\frac{W_{n1}}{L_a} \right)^2 \tag{13}$$

Finally, under high-level injection when

$$J < \frac{qn2D_a}{W_{n2}} \tag{14}$$

the total ON-state voltage can be approximated by

$$V_{\mathrm{ON}} = \frac{kT}{q} \ln \frac{W_{n2} n2 J}{2qD_a n_i^2} + \frac{W_T^2}{2\mu_a \sqrt{\tau_a}} \frac{\sinh(W_T/L_a)}{[\cosh(W_T/2) - 1](2qW_{n2}n2)^{0.5}} J^{0.5} \tag{15}$$

The first term in the expression for V_{ON} is due to the pn junction voltage drop; the second term is due to voltage drop across the conductivity-modulated center base region. In the preceding equations, D_P, L_P, μ_p and D_n, L_n, μ_n are diffusion constant, diffusion length, and mobility for holes and electrons, respectively; b is the ratio of D_n over D_P, D_a, L_a, μ_a and τ_a are the ambipolar carrier diffusion constant, diffusion length, mobility and lifetime under high-level injection. In addition, J is the device current density, T the temperature, and k the Boltzmann constant; $n1$, $p1$, $n2$, and $p2$ are the carrier concentrations, respectively, for the four layers of thicknesses of W_{n1}, W_{p1}, W_{n2} and W_{p2}; W_T is equal to the sum of W_{n1}, W_{p1}, W_{p2}.

Because for most practical high-power applications the current density through a photothyristor could be regarded as

in high-level injection, the ON-State voltage is clearly a very strong function of the total base width W_T and carrier lifetime τ_a. Another important parameter that depends heavily on the carrier lifetime is the holding current, the minimum current needed to keep a photothyristor in the ON state.

A General dc Model for Photothyristor Design and Analysis

Figure 5 shows the energy band diagram of a photothyristor under forward bias where the electron and hole currents are labeled for both the following discussion and derivation of a general dc model for photothyristor design and analysis.

Let us follow the flow of electrons getting into $N1$ layer from $P2$ region. It is clear that some of the electrons will be recombined in the $N1$ neutral region and the J1 junction interface, thereby giving rise to a recombination current I_{RN1} and resulting in a recombination current I_{RJ1}. The rest of the electrons will get through the forward-biased J1 junction and contribute to current I_{nD1}. All of these electrons are supplied by electrons overcoming the J3 junction, i.e., current I_{nD3}, plus those generated in the reverse-biased J2 junction, which is denoted as the generation-recombination current I_{GR}. In short, the electron current continuity equation takes the form of

$$I_{RN1} + I_{RJ1} + I_{nD1} = I_{nD3} + I_{GR} \tag{16}$$

where I_{nD1} is due to electrons overcoming the J1 junction. The total electron current I_{N3} supports the J3 junction recombination current I_{RJ3} and I_{nD3}, namely,

$$I_{N3} = I_{RJ3} + I_{nD3} \tag{17}$$

Notice that the electron current direction is opposite the electron flow direction as indicated in Fig. 5.

Similarly, the J3 junction hole diffusion current I_{P3} is supplied by holes generated in the J2 junction and by holes that diffused through the J1 junction without being recombined in the $N1$ neutral region. Thus, the hole current continuity equation can be established as

$$I_{pD1} - I_{RN1} + I_{GR} = I_{P3} \tag{18}$$

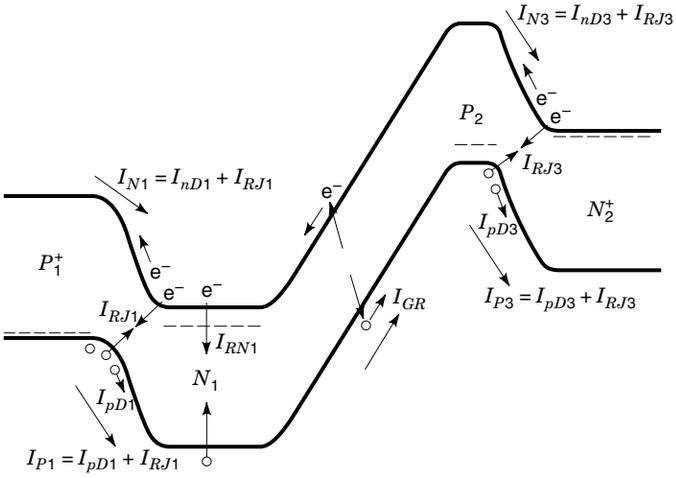

Figure 5. The energy band diagram of a photothyristor under forward bias showing the dominating electron and hole current components.

The I_{PJ3} supplies holes for the recombination current I_{RJ3} and the J3 junction diffusion current I_{pD3}, namely,

$$I_{P3} = I_{RJ3} + I_{pD3} \tag{19}$$

The values of these current components depend on the junction voltage $V1$, $V2$, $V3$ and $V_{\rm TOT}$, with $V_{\rm TOT}$ equal to the anode to cathode voltage across the photothyristor or

$$V_{\rm TOT} = V1 + V2 + V3 \tag{20}$$

By combining these equations, the electrical current components and the three junction voltage drops can be calculated when the photothyristor bias $V_{\rm TOT}$ is given. The total device current can then be calculated either as the total current leaving J3 junction

$$I = I_{RJ3} + I_{nD3} + I_{pD3} \tag{21}$$

or as the total current entering J1 junction:

$$I = I_{RJ1} + I_{nD1} + I_{pD1} \tag{22}$$

When light illumination exists and photons are mostly absorbed in the reverse-biased J2 junction, an extra current component, the photocurrent $I_{\rm photo}$, has to be considered. Clearly, the photocurrent $I_{\rm photo}$ simply adds to the generation-recombination current $I_{\rm GR}$ in the foregoing equations. The $I_{\rm photo}$ depends on a few parameters, including the optical input power $P_{\rm in}$, the absorption coefficient in the J2 junction α, the width of the center J2 region W_{J2} and an efficiency factor η to take into account the reflection and absorption outside the J2 junction

$$I_{\rm photo} = q\eta\frac{P_{\rm in}}{h\upsilon}[1 - \exp(-\alpha W_{J2})] \tag{23}$$

The detailed expression for each of the aforementioned diffusion, recombination and generation currents can be found in most introductory books on semiconductor devices (1).

For low-power photothyristor design, the internal optical efficiency, which describes how well the supplied carriers are converted to photons, can be calculated by the total radiative recombination current $I_{GR} + I_{N1}$ divided by the total current I. The emission of these photons can be spontaneous or stimulated, depending on the design of the active layer in the "i" region of the p-i-n structure of a photothyristor in the ON state.

Equivalent Circuit Model for Photothyristor Design and Analysis

Alternating current design and analysis can be carried out based on either a physical model or an equivalent circuit model. A physical model can be readily obtained by including the time-dependent junction capacitor charging current densities, $dQ1/dt$, $dQ2/dt$ and $dQ3/dt$ for junctions J1, J2 and J3, respectively, in the current continuity equations described in the last section. The junction charges $Q1$, $Q2$ and $Q3$ are equal to C_1V_1, C_2V_2 and C_3V_3 where C_1, C_2 and C_3 are the junction capacitances for junctions J1, J2 and J3, respectively. Transient analysis becomes possible using the modified current continuity equations. To include the effect of the interaction of photothyristors on other devices and circuit elements,

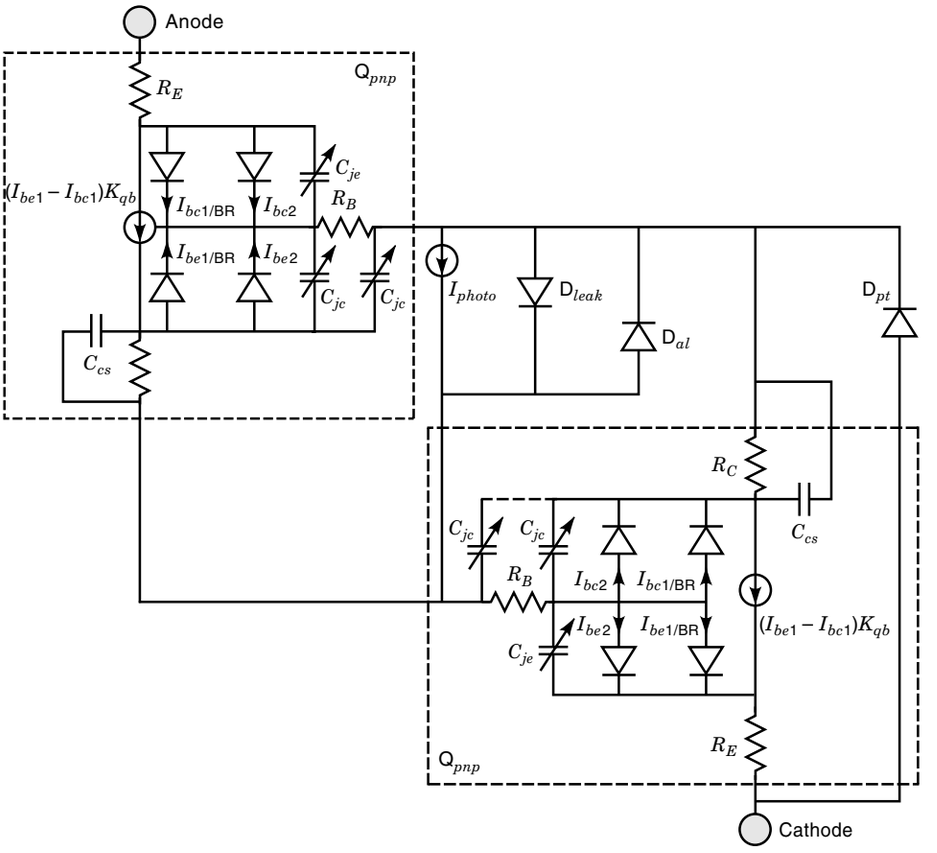

Figure 6. Equivalent circuit of a photothyristor including the effects of leakage current (D_{lk}), punchthrough (D_{pt}) and avalanche (D_{al}) breakdowns.

an equivalent circuit model can be used with the widely employed SPICE simulator. Figure 6 shows an equivalent circuit model for a pnpn photothyristor (8). It is based on the two-transistor model of the photothyristor already discussed. In the circuit, the photothyristor is modeled as a *pnp* transistor Q_{pnp} coupled to an *npn* transistor Q_{npn} through a forward-biased *pn* diode D_{pt} connected between the emitter and collector of the Q_{pnp} transistor, a reverse-biased *p–n* diode D_{al} connected between the base-collector junctions, and a forward-biased diode D_{lk} parallel to the base-collector junctions. Diodes D_{pt}, D_{al}, and D_{leak} are used to model the effects of punchthrough, avalanche and the OFF-state leakage current, respectively (8). A photocurrent source I_{photo} is included to model the effect of light absorption in the center J2 junction.

The required SPICE bipolar junction transistor parameters for the two transistors can be determined from current voltage curves obtained from standard device simulators such as PISCES (9) and SEDAN (10) among others.

Low-Power Photothyristors: An Example

A large amount of information on the performance of low-power photothyristors can be found in many photonic-related journals. Most discussions have focused on AlGaAs/GaAs based *PnpN* heterostructures. Little is available for InGaAsP/InP based photothyristors (11). For optical information processing, the key parameters are switching sensitivity and speeds. High sensitivity reduces the required optical energy for system applications and enhances cascadability and fan-out. The persistence of the ON state presents a major problem in improving the speed of photothyristors and the surface recombination currents at the periphery of the mesa in the space charge regions of the outer junctions J1 and J3 tend to reduce optical triggering sensitivity.

Effective approaches have been developed to reduce the surface recombination current and increase turn-off speed (12). When surface recombination current or the total leakage current is reduced, photothyristors become much more sensitive to the photocurrent generated by light absorption. One way to reduce surface recombination current uses the fact that the surface recombination current depends on the intrinsic carrier concentration n_i, as expressed by the following equation:

$$I_{SL} = qn_iSP(\Delta W/2)\exp(qV_E/(2kT)) \tag{24}$$

where n_i depends on $\exp(-E_g/(2kT))$ and E_g is the semiconductor bandgap depleted by a width of ΔW over which the maximum recombination rate occurs; S is the effective surface recombination velocity typically in the order of 10^7 cm/s; and P is the mesa perimeter. If the depletion region ΔW is largely in the wider bandgap AlGaAs outer layers, the total surface recombination current can be reduced by a factor of $\exp(\Delta E_g/(2kT))$ due to reduction in n_i value where ΔE_g is the difference between the bandgaps of AlGaAs and GaAs. This reduction factor can be as large as 1230 for $\Delta E_g = 0.37$ eV. Experiments have been performed (12) to confirm the effect of reducing the emitter layer doping concentration on the reduction of surface recombination current by measuring the dc

current gain of photogenerated current of a normal bipolar. *Npn* transistor with $N_{emitter} = 10^{18}$ cm^{-3} and $N_{base} = 2 \times 10^{17}$ cm^{-3} and of an *Npn* transistor with lightly doped $N_{emitter} = 10^{17}$ cm^{-3} and heavily doped $N_{base} = 10^{18}$ cm^{-3}. It is found that an identical current gain is reached at a 1000 times smaller base current level in the transistor with lightly doped emitter.

Enhanced sensitivity makes it possible to cascade similar photothyristors for optical signal processing; namely, a photothyristor can be switched on by illuminating it with a beam of light emitted from a similar photothyristor. This can be improved by embedding a photothyristor into a microoptical cavity so as to enhance the light absorption and emission due to optical resonance in the cavity.

Improving the turn-off speed of photothyristors is another key issue in the search for practical applications. The slow turn-off of a photothyristor occurs mostly because many excess carriers are stored in the center layers and these need to be removed before a photothyristor can be turned off. Two terminal photothyristors, which can be relatively simply integrated into 2-D arrays, are turned off by both reversing the bias polarity and excess carrier recombination. As already discussed, if the carriers in the center layers are not removed quickly after reversing the bias polarity the photothyristor can be turned on falsely due to enhanced dV/dt triggering. In switching a single photothyristor, enhanced dV/dt triggering means the full forward-bias voltage has to be applied even more slowly than when switching from equilibrium state if the excess charges stored in the center layers are not completely removed. In a differential pair, this means that when the forward bias is applied, it will always turn on the photothyristor that was on in the previous cycle. To remedy this problem, the light input to the intended winner must be greatly increased so as to generate more carriers in the intended winner compared to those carriers left in the previous winner (12).

To solve this problem, the excess carriers in the center layers of a *PnpN* photothyristor must be removed before triggering light can be applied. Although by adding an extra electrical gate contact to a two-terminal photothyristor the goal can be accomplished, device processing and array integration are substantially complicated.

An easier solution is to extract the excess carriers by changing bias polarity to negative instead of reducing the bias to zero. The center p and n layers should be designed such that they can be completely depleted by an appropriate reverse bias across the photothyristor. This is critical to fast turn off because the complete depletion of the central p and n layers leads to greatly increased extraction of electrons and holes from the center layers, which prevents the dV/dt triggering of the same photothyristor when the forward bias voltage is increased again.

Photothyristors designed based on this principle have been reported to have much a faster turn-off speed. One of these device structures grown by molecular beam epitaxy on n^+-GaAs substrate has a 1 μm 1 $\times$ 10^{18} cm^{-3} doped N-$Al_{0.05}Ga_{0.95}As$ on top of a 1.5 μm n^+-GaAs buffer layer, followed by a 0.17 μm 2 $\times$ 10^{17} cm^{-3} p-GaAs, a 0.17 μm 2 $\times$ 10^{17} cm^{-3} n-GaAs, a 0.28 μ 1 $\times$ 10^{19} cm^{-3} P-$Al_{0.2}Ga_{0.8}As$, and a 0.02 μm 2 $\times$ 10^{19} cm^{-3} p-GaAs as the contact layer (12). Deep mesas (0.9 μm) of 28 $\times$ 42 μm^2 were defined by wet etching and the top anode contact pad of Au/AuZn defined by liftoff has an area of 25 $\times$ 12 μm^2. The static forward breakover voltage of the fabricated photothyristors was in the range of 2.7 V. The turn-off time of such photothyristors has been measured with the voltage pulse cycle applied over a 100 Ω resistor.

In the experiment, the photothyristor is first switched on using a high positive bias, followed by the application of a negative voltage pulse V_{neg} of various amplitudes and durations t_{neg} to extract excess carriers in the center layers. The voltage across the photothyristor is then changed to V_{pos}, which is the threshold for the photothyristor to turn on within 1 μs; this should be considered as a dynamic breakover voltage (12); V_{pos} depends on the excess carriers left in the central layers. The larger the amount of excess carriers left in the central layers after the extraction pulse V_{neg}, the faster the *Pn* and *pN* junctions become forward biased and, hence, the smaller the V_{pos} at which the photothyristor turns on. The dependence of the critical V_{neg} on the V_{pos} is shown in Fig. 7 where it is seen that there is a sharp increase in V_{pos} for V_{neg} in excess of the -5.5 V, which corresponds to approximately a complete depletion of the center n-layer for t_{neg} equal to 10 ns or less. Because of the substantially lower hole mobility, the hole diffusion current is not sufficient to deplete the center p-layer completely until V_{neg} is equal to around -7.5 V, under which both n- and p-layers are depleted and V_{pos} becomes independent of the duration of carrier extraction pulse t_{neg} and is equal to the static forward breakover voltage of around 2.7 V. Theoretical simulation of the energy band diagram, shown in Fig. 8, confirms the depletion of the center n-layer at around -6 V (compared to experimental value of -5.5 V) and the complete depletion of both n- and p-layers at -9 V (compared to the observed -7.5 V).

The optical energy needed for correct switching of a photothyristor pair has also been investigated using a *PnpN* structure similar to the aforementioned device. Figure 9 shows the optical triggering energy needed for correct switching as a function of the bite rate. Optical energy of as low as 7.4 fJ or a specific optical energy of 12 aJ per μm^2 photothyristor area has been achieved.

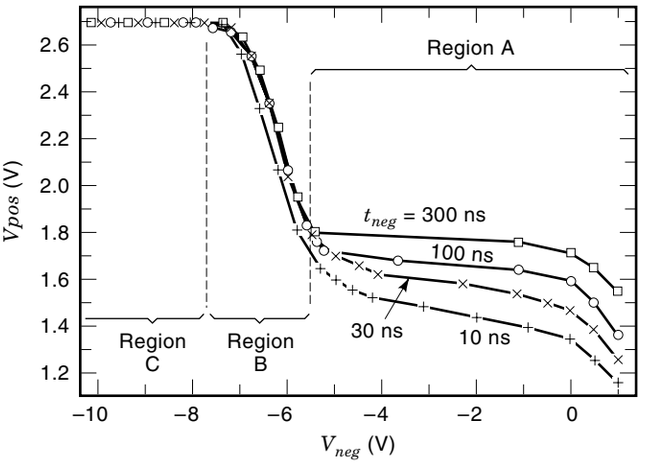

Figure 7. Experimental results of dependence of dynamic forward breakover voltage V_{pos} on the amplitude and duration of carrier extraction pulse V_{neg}. [After M. Kuijk et al., *Appl. Phys. Lett.,* **64** (16): 2074, 1994. Reprinted with permission.]

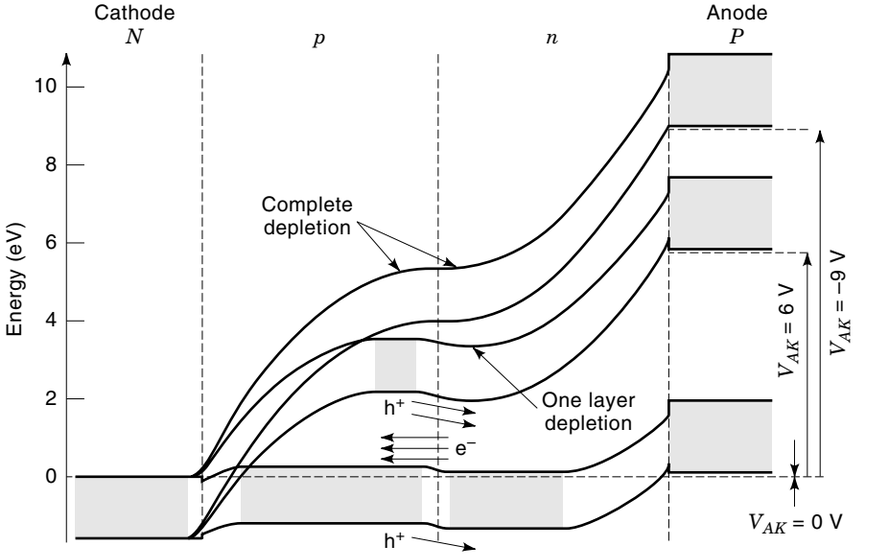

Figure 8. Energy band diagram of the photothyristor under zero, −6 V and −9 V bias showing depletion of *n*-layer at −6 V and total depletion of *n* and *p* layers at −9 V. [After M. Kuijk et al., *Appl. Phys. Lett.,* **64** (16): 2075, 1994. Reprinted with permission.]

High-Power Photothyristors: An Example

Power switching devices, in particular, the pnpn-based power thyristors, are the key component for many power electronic applications. While almost all of the power devices are currently based on Si, its intrinsic material property, i.e., its small bandgap, makes it difficult to be used above 120°C. To overcome this problem, wider bandgap materials have to be employed. The GaAs material system is a mature and ideal candidate for power switching applications at temperatures above 120°C. The intrinsic carrier concentration for GaAs at 290°C is the same as the intrinsic carrier concentration for Si at 120°C, which suggests that the possible operating temperature for GaAs photothyristors could be as high as 290°C. In addition to being able to operate at higher temperatures, GaAs-based power photothyristors can be expected to block much higher voltages because semiinsulating (SI) GaAs material is readily available in GaAs but not in Si. By "inserting" a semiinsulating GaAs into a conventional pnpn photothyristor structure, the resulted *pn-i-pn* photothyristor is capable of blocking much higher voltage as compared to those photothyristors formed by diffusion or grown epitaxially. By employing the wider bandgap AlGaAs as the optical window, the AlGaAs/GaAs-based *pn-i-pn* photothyristor becomes very sensitive to optical triggering when compared to the widely studied bulk photoconductive semiconductor switches (PCSS) (13). Another advantage is the higher turn-on and turn-off speeds in comparison to silicon-based power devices (14,15).

The first AlGaAs/GaAs heterostructure photothyristor using SI-GaAs as the voltage blocking layer was reported in 1993 (14). It was observed that even a light-emitting diode (LED) operated in the milliwatt power range can be used to turn on a correctly designed AlGaAs/GaAs high voltage photothyristor in a very smooth fashion (13). In addition to the lower energy required, electron and hole pairs are optically generated deeper inside the photothyristor rather than the near the metal contact region on the surface as is the case for a GaAs homojunction photothyristor. This reduces the possibility of either filament formation or surface breakdown, which is one of the major reasons for the greatly reduced power handling capability and lifetime of PCSS.

A typical $Al_{0.3}Ga_{0.7}$ As/GaAs high-power photothyristor structure grown by molecular beam epitaxy is shown in Fig. 10, where LT-GaAs stands for GaAs grown at a low temperature of 200°C. The recessed circular ohmic contacts have a

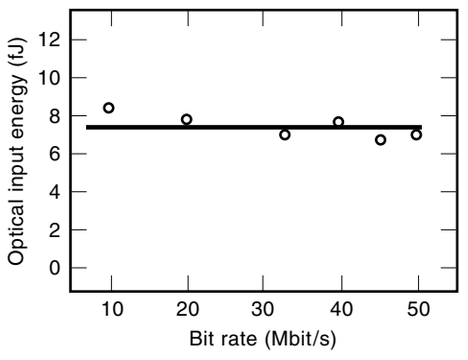

Figure 9. Optical input energy needed for correct switching as a function of signal bit rate. [After B. Knupfer et al., *Electronics Lett.,* **31** (6): 486, 1995. Reprinted with permission.]

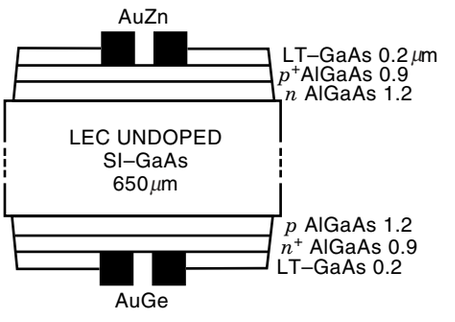

Figure 10. The cross-sectional view of an $Al_{0.3}Ga_{0.7}As$/GaAs based high-power photothyristor structure grown by MBE where LT-GaAs stands for GaAs grown at a low temperature of 200°C. [After Jian H. Zhao et al., *IEEE Trans. Electron Devices,* **41** (5): 820, 1994. Reprinted with permission.]

diameter of 0.5 cm, with an optical aperature of 0.1 cm in diameter. The photothyristor has a junction area of 0.79 cm^2 on both sides. The N^+P and P^+N doping concentrations are 1×10^{18} $cm^{-3}/3 \times 10^{17}$ cm^{-3} and 5×10^{18} $cm^{-3}/1 \times 10^{17}$ cm^{-3}, respectively.

Two types of measurements on these types of photothyristors can be done to characterize the switching performance. One is current-voltage (*I-V*) characteristics under low field using 50 ohms coaxial cable for differential voltage and current monitoring. The low field bias measurement can be used to observe and confirm the thyristor-like action of carrier injection from the P^+N and N^+P emitters. In the second type of measurement, the photothyristor switched-current waveforms (*I-t* relationship) and the voltage waveforms across the device (*V-t* relationship) under high fields can be measured directly using special current and voltage probes. These measurements can help determine the turn-on time di/dt and the maximum current capability of the photothyristor, all as a function of the blocking voltage. In these high-field dynamic current response measurements, low inductance connections should be used to connect the device to the measurement circuit and a special low-inductance current viewing resistor (CVR) needs to be used to monitor the switched-current through the photothyristor.

When the forward-bias field is low, laser triggering first generates a linear photocurrent as a direct and fast response to the laser beam absorption, followed by a much larger current conduction due to carrier injection from the P^+N and N^+P emitters. Both amplitude and duration of this current conduction depend largely on the thickness of SI-GaAs and the bias condition.

Under high-field bias, the carrier injection by the two emitters has a much shorter delay time after the laser triggering. Shown in Fig. 11(a) are the voltage waveforms across the photothyristor without (curve a) and with (curve b) laser triggering using the left vertical scale, 500 V/division, and the switched-current through the device with laser triggering using the right-hand side vertical scale, 20 A/division. The fiber-optical coupling of 0.05 μJ GaAs laser light is through the P^+-side of the optical aperture. The time scale is 500 ns/division. In this figure, the voltage across the device is seen to charge up to 1625 V and the laser is fired 1.75 μs into a 2.75 μs charging pulse. The switched-current increases rapidly when the device turns on. Voltage across the device drops rapidly to about 370 V and the current increases from zero to 100 A as shown in Fig. 11(b). The photothyristor does not latch on and the current decreases in less than 25 ns to zero, which makes the device an excellent high-power switch for generating narrow high-power pulses. The fine scale used in Fig. 11(b) shows clearly the linear photoconductive response of less than 20 A current as a shoulder on the left-hand side of the current waveform as well as a very fast risetime due to carrier injection from the P^+N and N^+P junctions.

Figure 12(a) and (b) shows the switched-current as a function of time for a photothyristor tested under different forward blocking voltages with the laser beam illuminated on the P^+-side aperture. Curves a through i correspond to forward blocking voltages of 2120, 2020, 1940, 1840, 1850, 1780, 1600, 1400, and 950 V, respectively. The small and broad first peaks in Fig. 12(b) and the almost overlapped low shoulder on the left-hand side of peaks in Fig. 12(a) are the linear photoconductive response currents. The second peaks on the

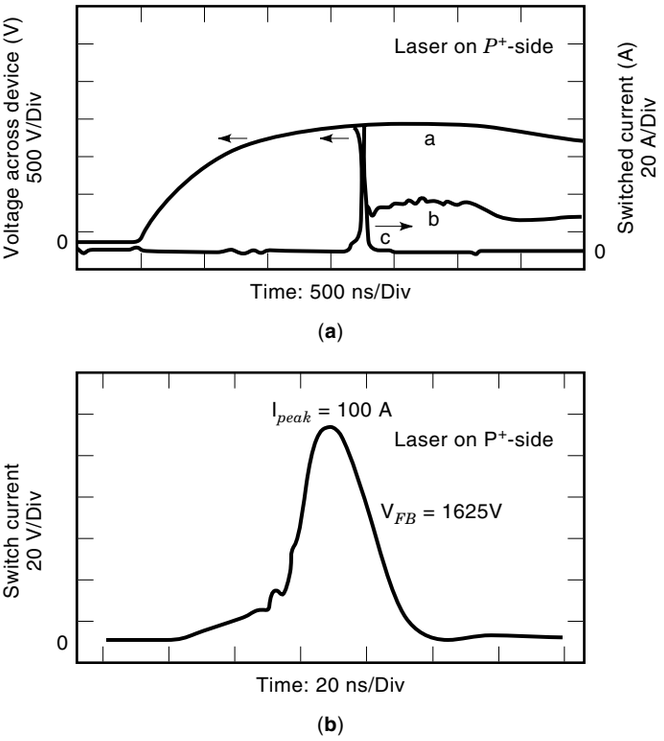

Figure 11. (a) The voltage waveforms across the 1625 V biased photothyristor without (curve a) and with (curve b) laser triggering using the left-hand side vertical scale, 500 V/division, and the switched-current through the device with laser triggering using the right-hand side vertical scale, 20 A/division. (b) Detailed current waveform showing the 100 A switched current. The fiber-optical coupling is through the P^+-side of the optical aperture. [After Jian H. Zhao et al., *IEEE Trans. Electron Devices,* **41** (5): 821, 1994. Reprinted with permission.]

right-hand side are results of P^+N and N^+P junction carrier injections induced by the first peaks. Figure 13 shows the forward bias device energy band diagram, which helps illustrate the concept of the carrier injections. In specific, the P^+N junction on the left-hand side injects holes into the SI-GaAs when the forward bias across it is increased. The N^+P junction on the right-hand side, however, injects electrons into the SI-GaAs when the forward bias increases. The injected holes and electrons help the turn-on of the devices. For a given blocking voltage, this increase of forward bias across the P^+N and N^+P junctions is transferred from the voltage across the SI-GaAs layer due to laser illumination. Of course, a higher-level carrier injection will take place if the initial blocking voltage is higher. Higher-level injections under higher blocking voltages lead to higher switched-current amplitudes. Figure 12 also shows that for high blocking voltages the generated current pulses have about the same full-width half-maximum (FWHM) of less than 25 ns. The turn-off time is about 15 ns, which is to be compared with a few hundred microseconds to milliseconds turn-off times for Si-based thyristors having similar power capability.

The much lower linear photoconductive peak current I_{photo} and the photothyristor maximum switched-current I_{max} are shown in Fig. 14 for a clear comparison of the photothyristor advantages over the conventional photoconductive switches. The maximum photothyristor switched-current reaches 156

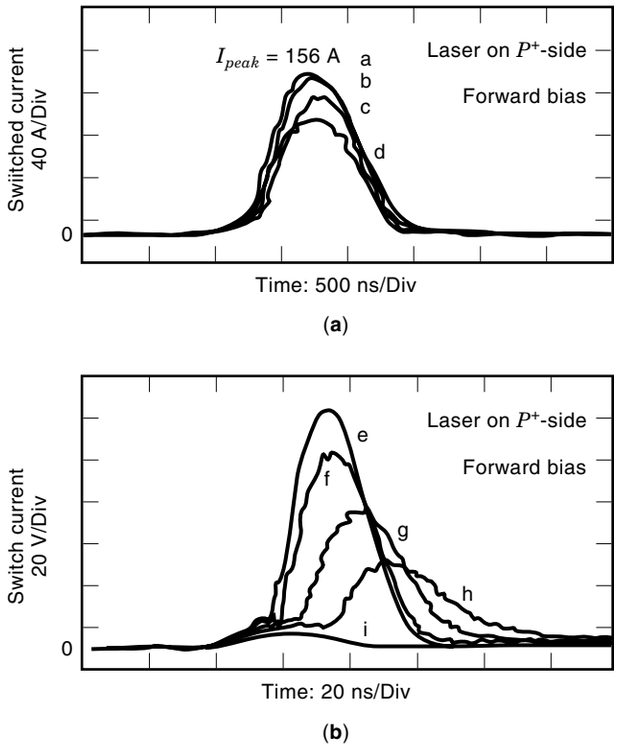

Figure 12. The switched-current as a function of time for the photothyristor tested under different forward blocking voltages with the laser beam illuminated on the P^+-side aperture. Curves a through i correspond to forward blocking voltages of 2120, 2020, 1940, 1840, 1850, 1780, 1600, 1400, and 950 V, respectively. (a) Overlapped low shoulder, left-hand side of peaks indicates linear photoconductive response currents. (b) Small and broad peaks indicate same currents. [After Jian H. Zhao et al., *IEEE Trans. Electron Devices,* **41** (5): 822, 1994. Reprinted with permission.]

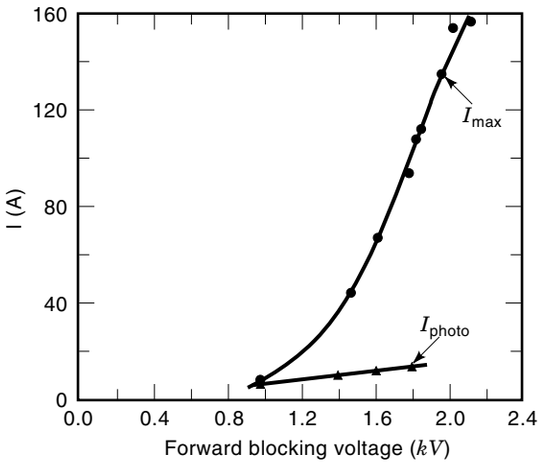

Figure 14. The linear photoconductive peak current I_{photo} and the photothyristor maximum switched-current I_{max} as a function of the photothyristor blocking voltage showing the clear advantage of photothyristors over the conventional linear photoconductive switches. [After Jian H. Zhao et al., *IEEE Trans. Electron Devices,* **41** (5): 823, 1994. Reprinted with permission.]

A, which is close to an order of magnitude higher than the linear photocurrent when extrapolated to 2120 V bias. A much larger difference in the switched-current amplitude at a 40 to 50 kV bias range can be expected. The scale-up of the photothyristor can be accomplished by increasing the SI-GaAs layer thickness. This substantial increase in current handling capability is one of the most important aspects of this high-power photothyristor. In order to switch high current using linear photoconductive switches, a physically large high-power laser is needed because most of the electrons and holes for current conduction have to be generated by photon absorption. Operating photoconductive switches in the lock-on mode (6) can reduce the required optical energy for triggering to microjoule range, but lock-on, as the terminology implies, locks the switch in the on-state for a very long time, making it difficult to use in opening switches. Additionally, switches that are operated in the lock-on mode normally have a much shorter device lifetime. Using this P^+N-i-PN^+ photothyristor, however, most of the electrons and holes for current conduction are due to the P^+N and N^+P injections, thereby making it possible for the photothyristor to conduct the same amount of maximum current when triggered by laser beams of 0.3 and 0.05 μJ. It has been shown that even an LED in the milliwatt power range can be used in smooth turn-on of the photothyristor (13). This makes it possible to fabricate portable compact high-power pulsers by integrating the photothyristors and miniature semiconductor lasers on the same chip. Another advantage, in comparison to the bulk photoconductive switch, is the improved device reliability and, lifetime because the metal contacts on P^+ and N^+ are excellent ohmic contacts; this eliminates the fast contact degradation and local field enhancement around poor metal contacts. Local field enhancement can greatly reduce device lifetime through the formation of filaments or surface breakdown. Theoretical and experimental results have shown that the local field enhance-

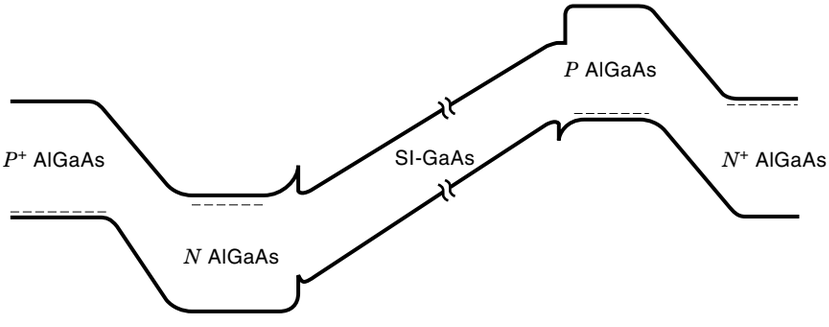

Figure 13. The forward biased photothyristor energy band diagram where P^+N and N^+P junctions inject holes and electrons, respectively, into the SI-GaAs. [After Jian H. Zhao et al., *IEEE Trans. Electron Devices,* **41** (5): 822, 1994. Reprinted with permission.]

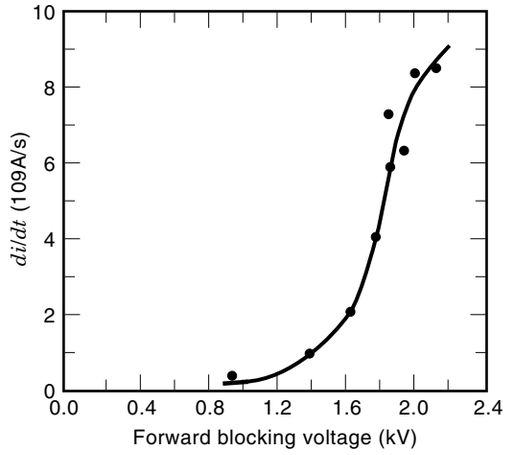

Figure 15. The rate of rise of switched-current as a function of the photothyristor blocking voltage. [After Jian H. Zhao et al., *IEEE Trans. Electron Devices,* **41** (5): 823, 1994. Reprinted with permission.]

ment is eliminated in contacts on heavily doped layers under high field intensity (16). The low pulse repetition frequency of bulk photoconductive switches can be solved with the photothyristor because the light source for triggering, the semiconductor lasers, can be modulated at frequencies orders of magnitude higher than the conventional high-power solid state or gas lasers.

The important quantity di/dt, which characterizes the turn-on of the photothyristors and is defined as the difference between 90% of the peak current and 10% of the peak current divided by the corresponding time interval, is shown in Fig. 15. The maximum di/dt value is around 8.5×10^9 A/s. Much higher di/dt values are possible for higher blocking voltage photothyristors.

This AlGaAs/GaAs-based P^+N-i-PN^+ photothyristor is potentially an ideal candidate for realizing portable and compact ultrahigh-power pulsed switches and for integrating the photothyristors and miniature semiconductor lasers on the same chip because the majority of electrons and holes for current conduction through the thick SI-GaAs are injected by the P^+N and N^+P emitters; laser illumination is used only as a trigger for the carrier injection. High repetition rate becomes possible using this type of photothyristor because a compact and high-speed laser source can be used for optical triggering.

APPLICATIONS AND FUTURE DIRECTIONS

Lower-Power Photothyristors

Low-power photothyristors have been investigated for many potential photonic applications including optical neural nets and pattern recognition, optical parallel processing, reconfigurable optical interconnection, low power consumption dynamic memories, smart pixels, and basic optical logic gates of NAND, NOR, AND and OR for optical computing. Using advanced epitaxial technologies such as low pressure-metal-organic chemical vapor deposition (LP-MOCVD), cascadable photonic switches have also been realized based on the monolithic integration of an ALGaAs/GaAs multiquantum well vertical-cavity surface emitting laser (VCSEL) and an AlGaAs/GaAs *PnpN* photothyristor. The VCSEL and *PnpN* structures can be independently optimized for optical switching, logic and memory functions. Optical switching with high gain (30,000), high contrast (30 dB), low switching power (11 nW) and latching memory have been achieved (17). Based on similar integrated structures, more complex switch nodes with increased functionality that are capable of performing optical logic and routing in a dynamically programmable manner have also been realized (18).

For optical net and pattern recognition applications, the location of the maximum light intensity in a 2-D spatially distributed light pattern needs to be determined. A monolithic 2-D array of photothyristors connected in parallel has been used to perform the task based on the winner-takes-all principle (12). The photothyristor located at the place illuminated by the strongest light intensity turns on after the application of a short-voltage pulse and emits light typically in the range of microwatts. The maximum intensity location can be identified within the range of approximately 100 ns after the application of turn-on voltage pulse. The input light pattern can be of very short duration applied a short time before the voltage pulse. With a difference of 80 pJ, differential switching allows for the accurate identification of maximum intensity location. To determine the maximum dose location, all optical energy incident on each photothyristor should be integrated. Depending on the device structure and bias conditions, the effect of optical energy within 1 ms before the application of the triggering voltage pulse has been observed to accumulate. By varying the delay time between the optical illumination and the application of the triggering voltage pulse, the photothyristor at the location of the maximum dose exposure turns on and the location is identified.

For a Boolean logic gate application such as an inverter, a photothyristor is connected in parallel with a VCSEL. Without optical illumination, the photothyristor, biased at a voltage slightly below the forward breakover voltage through a common resistor shared with a VCSEL, is in the OFF state. The total current in the circuit is therefore bypassed by the VCSEL, resulting in coherent laser light emission from the VCSEL. When the photothyristor is illuminated, the turn-on voltage of the photothyristor is reduced to a voltage below the threshold voltage of the VCSEL. This causes the VCSEL to turn off. The logic function of this gate is inverting and the optical contrast, the ratio of optical output power in the dark to optical output power under illumination can be very high. The NOR and NAND gates can be implemented using multiple photothyristor input ports. In the NOR gate configuration, multiple photothyristors and a VCSEL are connected in parallel. For NAND gate implementation, multiple photothyristors are connected in series and then in parallel with a VCSEL.

Using a properly designed optical system, logic gates of NAND, NOR, AND or OR have also been realized using only differential pairs of photothyristors (19). A data rate of up to 50 MHz has been realized for transcription between neighboring differential pairs on a single wafer. By using a compact optical system that combines large diameter gradient index lenses with Fourier plane diffractive optics, a system has been implemented with three cascaded photothyristor stages with an element to array fan-out equal to three.

Currently, cascaded systems based on photothyristor differential pairs are capable of channel frequency of up to 5 MHz and 7 Gbit/s parallel bit rate. The prediction, based on the steady improvement of photothyristor technology, is that the near future 84 MHz channel frequency and 130 Gbit/s parallel bit rate will be possible. Ideally one would like to have high interconnection efficiency and a megahertz channel frequency in the hundreds as well as over 700 Gbit/s parallel bit rate.

High-Power Photothyristors

High-power photothyristors have many potential applications including high-power pulsed lasers, ultrawide-band impulse radars, high-power microwave and millimeter-wave systems, high voltage direct current (HDVC) power transmission, power generators, high repetition pulsed power sources, electric gun control due to the advantages of the optical isolation of gate triggering from the high-voltage bias circuitry and high-power and high-speed performance in comparison to conventional thyristors. For example, because of the isolation of gate triggering, circuitry from the high-voltage, high-power photothyristors can be stacked in series to handle very high voltages for HVDC power transmission over a long distance with improved transient stability and dynamic damping of the electrical system oscillations. In the late 1970s silicon based photothyristors rated 800 A average current and 2600 V peak repetitive blocking voltage have been reported and used for utilty control by stacking 24 pairs of reverse-parallel connected photothyristors in series. The utilty industry's first self-protected silicon photothyristor module was installed in 1986 on a 13.8 kV, 40 MVAR ac switch using 16 series-connected devices operating in one phase of a static var compensator (20).

In the areas of high pulsed repetitive power generation for the applications of electron beam generation, laser excitation, sterilization, nonthermal plasma treatment of hazardous gaseous waste and pollutants, and microwave generation, photothyristors (especially the high-speed ones) are expected to gain increased attention. An example of the application of high-speed power photothyristors as opening switches is the use of a photothyristor to transfer energy stored in an inductor L to a load R. In the simplest form of such an application, an inductor, a photothyristor and a load are connected in parallel. The inductor is charged with a current I over a long period of time compared to the time needed to transfer its energy to the load. Transfer of energy stored in the magnetic fields is accomplished by carrier recombination after the removal of illuminating light source, which opens the photothyristor and forces current through the load. The photothyristor must be very robust to survive the transients resulting from the sudden current interruption. In the simplest case, opening the photothyristor leads to a voltage V across the switch ranging from $I \times R$ to zero, depending on whether the opening is very fast or very slow. If the load has a parasitic inductor L_p, the voltage across the photothyristor can rise to a very high value of $L_p di/dt$. For RF power generation and pulsed accelerator applications, high-speed photothyristors based on advanced semiconductors should be used. Silicon-based photothyristors, however, are suitable for the long pulse mass launcher applications such as electric guns.

For stationary electromagnetic launchers (EML) and electrothermal chemical (ETC) gun applications, silicon-based photothyristors having superior performance have been evaluated (in comparison to plasma type switches) in a number of important areas such as lifetime, reliability and support. To realize a mobile system, however, the pulser must be operated at the highest power density possible. Measurements on prototype systems have shown that the size and weight of the switches are prohibitive. Because SiC promises a power density 10 to 100 times higher than that of silicon, future research should be concentrated on developing SiC based photothyristors (21) which will not only reduce both size and weight but also improve the reliability and lifetime in comparison to silicon-based photothyristors because SiC has a much higher thermal conductivity and may be operated at temperatures of well over 300 °C.

Future improvement to photothyristors for utility application depends on the development of photothyristors based on advanced wide bandgap semiconductors such as SiC. Due to its high electric field strength, high thermal conductivity and high temperature operation capability, SiC photothyristors could substantially reduce the power switch system size and cost and greatly improve reliability and lifetime. Towards this end, compact laser sources based on the wide bandgap semiconductors such as the GaN/AlGaN system should be developed for triggering SiC photothyristors. As is the case for all electrical and optical devices, the future direction for photothyristors is towards ever increasing performance criteria. The first critical parameter for high-power application is the minimum light energy needed for triggering; the desired reduction would be to the level of a single laser diode.

The dI/dt and dV/dt immunities are of critical importance for most high-power applications. Improvement of these parameters is constrained by the trade-off between the optical triggering sensitivity and the immunities. Novel structure and design topology need to be developed to further practical applications. High-speed operation and high-repetition rate are of great importance for impulse power switching and high-power radar applications. A trade-off exists between the speed and power capability due to the requirement of a thicker blocking layer for higher voltage. For applications over 120 °C, photothyristors based on wider bandgap semiconductors such as GaAs and AlGaAs should be developed. For applications over 290 °C, even wider bandgap materials should be employed.

To achieve the ultimate high-speed and high-power performance, SiC-based photothyristors should be investigated along with the development of a compact GaN-based light source for triggering. Compact pulsers based on this hybrid SiC/GaN technology should find much wider applications in the future.

BIBLIOGRAPHY

1. S. M. Sze, *Physics of Semiconductor Devices,* 2nd ed., New York: Wiley, 1981.
2. G. W. Taylor et al., A new double heterostructure optoelectronic switching device using molecular beam epitaxy, *J. Appl. Phys.,* **59** (2): 596–600, 1986.
3. K. Kasaharq et al., Double heterostructure optoelectronic switch as a dynamic memory with low-power consumption, *Appl. Phys. Lett.,* **52**: 679–681, 1988.
4. G. W. Taylor et al., Ledistor—a three-terminal double heterostructure optoelectronic switch, *Appl. Phys. Lett.,* **50** (6): 338–340, 1987.

5. S. Wang et al., Optical bistability in a pnpn GaAs/AlGaAs laser diode, *Solid State Electron.,* **30** (1): 53–57, 1987.
6. R. P. Brinkman et al., The lock-on effect in electron-beam-controlled gallium arsenide switches, *IEEE Trans. Electron Devices,* **38**: 1991.
7. M. Otsuka, The forward characteristic of a thyristor, *Proc. IEEE,* **55**: 1967, 1400–1408.
8. D. A. Suda, Theory and Design of pnpn Optoelectronic Devices, Ph.D. thesis, University of Colorado, p. 26, 1992.
9. M. R. Pinto et al., PISCES-IIB, Supplementary Report, Stanford Electronics Laboratories, Department of Electrical Engineering, Stanford University, 1985.
10. Z. Xu and R. W. Dutton, Sedan III: A general electronic material and device analysis program, Program Manual, Stanford University, July 1985.
11. W. Buchwald et al., A three terminal InP/InGaAsP optoelectronic thyristor, *IEEE Trans. Electron Devices* **41**: 620–622, 1994.
12. M. Kuijk et al., Depleted double-heterojunction optical thyristor, *Appl. Phys. Lett.,* **64** (16): 2073–2075, 1994.
13. J. H. Zhao et al., Sensitive optical gating of reverse-biased AlGaAs/GaAs optothyristors for pulsed power switching applications, *IEEE Trans. Electron Devices,* **40**: 817–823, 1993.
14. J. H. Zhao et al., Dynamic I-V characteristics of an AlGaAs/GaAs-based optothyristor for pulsed power-switching applications, *IEEE Electron Device Lett.,* **13** (3): 161–163, 1993.
15. J. H. Zhao et al., A novel high power optothyristor based on AlGaAs/GaAs for pulsed power switching applications, *IEEE Trans. Electron Devices,* **41**: 819–825, 1994.
16. W. R. Donaldson and L. Mu, The effects of doping on photoconductive switches as determined by electro-optic imaging, *Proc. SPIE,* **1632**: 81–87, 1992.
17. P. Zhou et al., Cascadable, latching photonic switch with high optical gain by the monolithic integration of a vertical-cavity surface-emitting laser and a pn-pn photothyristor. *IEEE Trans. Photonic Technol. Lett.,* **3**: 1009–1012, 1991.
18. J. Cheng, Monolithic optical switching technology for a programmable optical logic gate array, *Optics Laser Technol.,* **26** (4): 239–249, 1994.
19. H. Thienpont et al., Optical thyristor based subsystems for digital parallel processing: demonstrators and future perspectives, *Int. Conf. Massively Parallel Process. Using Opt. Interconnections (MPPOI), IEEE Proc. 1995,* 1995, pp. 228–238.
20. F. Cibulka, L. Crane, and J. Marks, Field evaluation of industry's first self-protected light-triggered thyristors, *IEEE Trans. Power Deliv.,* **5**: 110–115, 1990.
21. L. Kingsley et al., Silicon carbide optoelectronic switches, *Proc. SPIE,* **2343**, 114–120, 1995.

JIAN H. ZHAO
Rutgers, The State University of New Jersey
TERRY BURKE
United States Army

PHOTOVOLTAIC CELLS. See SOLAR CELLS.